Langmuir

Article

pubs.acs.org/Langmuir

Star-Shaped Trimeric Quaternary Ammonium Bromide Surfactants: Adsorption and Aggregation Properties

Tomokazu Yoshimura,*[,†] Takumi Kusano,[‡] Hiroki Iwase,[§] Mitsuhiro Shibayama,*[,‡] Tetsuya Ogawa,[⊥] and Hiroki Kurata[⊥]

[†]Research Group of Chemistry, Division of Natural Sciences, Nara Women's University, Kitauoyanishi-machi, Nara 630-8506, Japan

[‡]Institute for Solid State Physics, The University of Tokyo, Kashiwanoha, Kashiwa, Chiba 277-8581, Japan

[§]Comprehensive Research Organization for Science (CROSS), 162-1 Shirakata, Tokai, Ibaraki 319-1106, Japan

[⊥]Institute for Chemical Research, Kyoto University, Gokasho, Uji, Kyoto 611-0011, Japan

Supporting Information

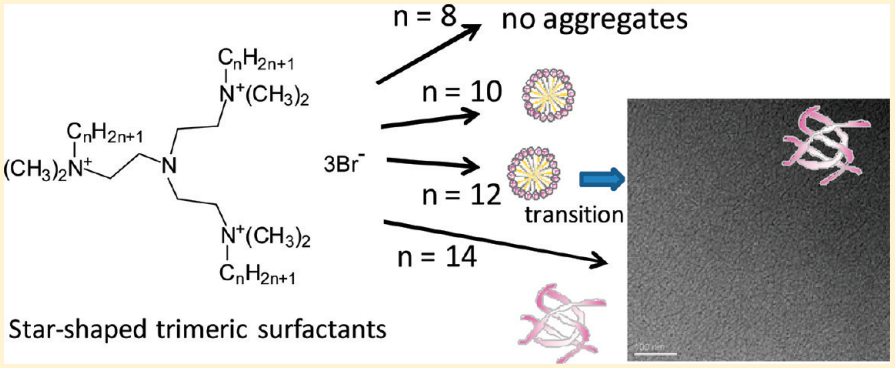

ABSTRACT: Novel star-shaped trimeric surfactants consisting of three quaternary ammonium surfactants linked to a tris(2-aminoethyl)amine core were synthesized. Each ammonium had two methyls and a straight alkyl chain of 8, 10, 12, or 14 carbons. The adsorption and aggregation properties of these tris(*N*-alkyl-*N*,*N*-dimethyl-2-ammoniumethyl)amine bromides ($3C_n$trisQ, in which *n* represents alkyl chain carbon number) were characterized by equilibrium and dynamic surface tension, rheology, small-angle neutron scattering (SANS), and cryogenic transmission electron microscopy (cryo-TEM) techniques. $3C_n$trisQ showed critical micelle concentrations (CMC) 1 order of magnitude lower than that of the corresponding gemini surfactants with an ethylene spacer and the corresponding monomeric surfactants. The logarithm of the CMC decreased linearly with increasing hydrocarbon chain length for $3C_n$trisQ. The slope of the line, which is well-known as Klevens equation, was larger than those of the monomeric and gemini surfactants; however, considering the total carbon number in the chains, the slope was shallower than the monomeric and was close to the gemini. Through the results such as surface tensions at the CMC (32−34 mN m^{-1}) and the parameters of standard free energy, CMC/C_{20} and pC_{20}, it was found that $3C_n$trisQ could adsorb densely at the air/water interface despite the strong electrostatic repulsion between multiple quaternary ammonium headgroups. Moreover, dynamic surface tension measurements showed that the kinetics of adsorption for $3C_n$trisQ to the air/water interface was slow because of their bulky structures. Furthermore, the results of rheology, SANS, and cryo-TEM determined that $3C_n$trisQ with $n = 10$ and 12 formed ellipsoidal micelles at low concentrations in solution and the structures transformed to threadlike micelles with very few branches for $n = 12$ as the concentration increased, but for $n = 14$ threadlike micelles formed at relatively low concentrations.

INTRODUCTION

Recently, oligomeric surfactants with multiple hydrophobic groups and multiple hydrophilic groups in a molecule have become attractive as a new class of surfactants. Gemini or dimeric surfactants, the simplest oligomeric surfactants, contain two hydrophobic and two hydrophilic groups, and they have unusual and unique properties that merit synthetic, physicochemical, and applied investigations.[1,2] Gemini surfactants consist of conventional monomeric surfactant fragments connected together with spacer group near hydrophilic headgroups. Extending gemini surfactants furnishes trimeric and tetrameric surfactants. In the first report on trimeric surfactants, Zana et al. synthesized quaternary ammonium-type surfactants with three dodecyl chains and three ammonium headgroups connected by two propylene spacer groups.[3,4] By changing the counterions (Br vs Cl), they investigated the surfactants' critical micelle concentrations (CMC), micelle ionization degrees, and micelle aggregation numbers. Esumi,

Received: March 22, 2012
Revised: May 26, 2012
Published: May 29, 2012

Ikeda, and Zana prepared similar trimeric surfactants with different spacer chain lengths (s = 2^5 and 6^6), spacers (2-hydroxypropylene),[7] and hydrocarbon chain lengths (C_8–C_{12}),[8] and their adsorption and aggregation properties were investigated in detail. For instance, trimeric surfactants have much lower CMCs than those of the corresponding monomeric and gemini surfactants, and CMC increases with spacer length. The micelle aggregation number also decreases with increasing spacer chain length in a trend similar to that of gemini surfactants. In addition, cryo-TEM observations showed that branched threadlike micelles form for s = 3, and spheroidal micelles form for s = 6. Laschewsky et al. also synthesized trimeric surfactants with rigid spacer groups such as *trans*-butenylene, *m*-xylylene, and *p*-xylylene, and their surface tension, viscosity, foaming, solubilizing capacity, and micelle aggregation numbers were studied and compared to those of the corresponding gemini and tetrameric surfactants.[9,10] Furthermore, Wang et al. synthesized two types of trimeric surfactants with amide groups in the spacers and reported their fundamental properties and vesicle-to-micelle transitions in solution.[11,12] There are also some reports concerning anionic[13−15] and nonionic[16] trimeric surfactants, in addition to the cationic ones mentioned above. We also reported the synthesis and properties of star-shaped anionic trimeric surfactants, whose spacer groups radiate from a central tertiary amine, derived from tris(2-aminoethyl)amine.[15] However, there are still relatively few reports on trimeric surfactants compared with gemini. Trimeric surfactants are more difficult to synthesize, and the starting materials are more expensive. Additionally, the relationships between structures with varying numbers of hydrocarbon chains and chain lengths are not yet clear.

In this paper, we describe the synthesis of novel quaternary ammonium star-shaped trimeric surfactants, tris(*N*-alkyl-*N*,*N*-dimethyl-2-ammoniumethyl)amine bromides ($3C_n$trisQ, where n represents alkyl chain carbon number of 8, 10, 12, and 14). $3C_n$trisQ was derived from tris(2-aminoethyl)amine and is shown in Figure 1. Several adsorption and aggregation properties of the surfactants were evaluated including equilibrium and dynamic surface tension, rheology, small-angle neutron scattering (SANS), and cryogenic transmission electron microscopy (cryo-TEM).

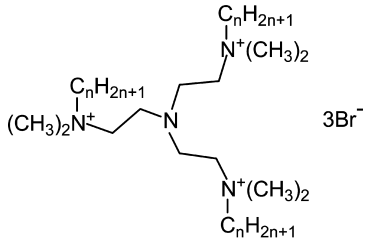

3C$_n$trisQ (n = 8,10,12,14)

Figure 1. Chemical structures of star-shaped quaternary ammonium bromide trimeric surfactants, $3C_n$trisQ.

EXPERIMENTAL SECTION

Materials. Tris(2-aminoethyl)amine, *n*-octyl iodide, *n*-decyl iodide, *n*-dodecyl iodide, and *n*-tetradecyl bromide were obtained from Tokyo Chemical Industry Co., Ltd. (Tokyo, Japan). Formaldehyde (35%) and formic acid (85%) solutions were purchased from Nacalai Tesque. Inc. (Kyoto, Japan). Acetone, ethanol, ethyl acetate, hexane, methanol, hydrochloric acid (35%), and sodium hydroxide were obtained from Kanto Chemicals Co., Inc. (Tokyo, Japan). All chemicals were reagent-grade commercial materials and used without further purification.

Synthesis of Tris(*N*,*N*-dimethyl-2-aminoethyl)amine. Tris(2-aminoethyl)amine (48.6 g, 0.33 mol) was added slowly to a stirred solution of formaldehyde (6.1 mol) and formic acid (5.6 mol) at room temperature, and the mixture was refluxed for 12 h. Concentrated hydrochloric acid was added to the mixture, and the solution was heated on a water bath for 3 h. After the solution was concentrated on a rotary vacuum evaporator, the residual solid was washed twice with methanol and dried under reduced pressure to give tris(*N*,*N*-dimethyl-2-aminoethyl)amine hydrochloride as a white solid in 65% yield. The data of ^{1}H NMR and elemental analysis are shown in Supporting Information.

Synthesis of Tris(*N*-alkyl-*N*,*N*-dimethyl-2-ammoniumethyl)-amine Bromides ($3C_n$trisQ). Tris(*N*,*N*-dimethyl-2-aminoethyl)-amine hydrochloride (10.0 g, 0.029 mol) was added slowly to 400 mL of methanol containing sodium hydroxide (16 g), and the solution was stirred with heating for 2−3 h. After the solvent was removed by evaporation, acetone was added to the residue, and the solution was filtered to remove the inorganic precipitate. The evaporation of acetone yielded tris(*N*,*N*-dimethyl-2-aminoethyl)amine as a brown liquid. Next, *n*-octyl iodide (n = 8), *n*-decyl iodide (n = 10), *n*-dodecyl iodide (n = 12), or *n*-tetradecyl bromide (n = 14) (0.174 mol) was added to a stirred solution of tris(*N*,*N*-dimethyl-2-aminoethyl)amine in about 200 mL of ethanol. The mixture was refluxed for over 40 h. After the solvent was evaporated under reduced pressure, the residue was washed several times first with ethyl acetate and then with hexane and recrystallized from mixtures of ethyl acetate and ethanol to give each tris(*N*-alkyl-*N*,*N*-dimethyl-2-ammoniumethyl)amine iodide or bromide as white solids. The yields were 74%, 76%, 82%, and 45% for n = 8, 10, 12, and 14, respectively.

To prepare bromides for n = 8, 10, and 12, the iodide compounds were dissolved in methanol and passed through a column of Dowex 1-X8 anion-exchange resin (exchanged from Cl to Br form, 50−100 mesh). After the eluant was evaporated under reduced pressure, the residue was washed with ethyl acetate, recrystallized from mixtures of ethyl acetate and ethanol, and dried under reduced pressure, yielding $3C_n$trisQ (n = 8, 10, and 12) as white solids. The data of ^{1}H NMR and elemental analysis are shown in Supporting Information.

Measurements. Except when used in the SANS experiment, the surfactant solutions were prepared using Milli-Q Plus water (resistivity = 18.2 MΩ cm) and the measurements were performed at 25 ± 0.5 °C. The surfactant solutions for SANS measurement were prepared with deuterium oxide (D_2O), and the measurements were performed at 28 ± 0.5 °C.

General Methods. The electrical conductivity measurements were performed with a CM-30R TOA electrical conductivity meter to determine Krafft temperature and CMC. The surface tensions of aqueous solutions of the star-shaped trimeric surfactants were measured with a Krüss K122 tensiometer using the Wilhelmy plate technique. The surface excess concentration (Γ) in mol m^{-2} and the area occupied by each molecule (A) of each trimeric surfactant at the air/solution interface were calculated using the classic Gibbs adsorption isotherm equations,[17] $\Gamma = -(1/iRT)(\mathrm{d}\gamma/\mathrm{d}\ln C)$ and $A = 1/(N\Gamma)$. Here, γ is the surface tension, C the surfactant concentration, R the gas constant (8.31 J K^{-1} mol^{-1}), T the absolute temperature, and N Avogadro's number. The value of i in the equation for the trimeric surfactants is taken to be 4, which is the number of possible species assuming complete dissociation in solution.

The fluorescence measurements of the star-shaped trimeric surfactants were performed with a Hitachi 650-10S fluorescence spectrophotometer. The dynamic surface tensions of the star-shaped trimeric surfactant solutions were measured with a Krüss BP2 bubble-pressure tensiometer. The rheological experiments were performed on a stress-control rheometer (MCR-501, Anton Paar, Austria) in viscosity measurement mode. The details of these measurements are shown in Supporting Information.

Small-Angle Neutron Scattering (SANS). SANS experiments were performed using the SANS-U instrument owned by the Institute for

dx.doi.org/10.1021/la301220y | *Langmuir* 2012, 28, 9322−9331

Solid State Physics at the University of Tokyo placed at research reactor JRR-3 of the Japan Atomic Energy Agency, Tokai, Japan. The neutron wavelength was 7.0 Å with a wavelength distribution ($\Delta\lambda/\lambda$) of ca. 0.1 and sample-to-detector distances of 1 and 8 m. The scattering profiles $I(q)$ were obtained in the q-range 0.005 to 0.3 Å^{-1}.

To determine the shape of the micelles quantitatively, the SANS data were fit to a model. In general, the scattering function for an assembly of particles is given by

$$I(q) = n(\Delta\rho)^2 V^2 P(q) S(q) \quad (1)$$

where n is the number of particles per unit volume in solution, $\Delta\rho$ the scattering contrast, and V the volume of a single particle. $P(q)$ and $S(q)$ are the form factor and the interparticle structure factor, respectively. Here, the form factor $P(q)$ for an ellipsoidal shape is given by

$$P(q) = 9\int_0^1 \left(\frac{J_1(qR_s)}{qR_s}\right)^2 \mathrm{d}x \quad (2)$$

where $J_1(x)$ is the first-order Bessel function of x. The R_s is defined as

$$R_s = R_1[1 + x^2(u^2 - 1)]^{1/2} \quad (3)$$

where R_1 and u are the minor axis and the axial ratio, respectively. Note that for spherical micelles, $u = 1$. The interparticle structure factor ($S_{HP}(q)$) was calculated by using a model proposed by Hayter and Penford.[18] This structure factor, taking into consideration the particle-shape ($S'(q)$), is given by

$$S'(q) = 1 + |\langle F(q)\rangle|^2/\langle |F(q)|\rangle^2 (S_{HP}(q) - 1) \quad (4)$$

where $F(q)$ is the scattering amplitude.

The form factor $P(q)$ for rod particles with a radius of R_c and length of L is given by

$$P(q) = \int_0^{2/\pi} \left[\frac{2J_1(qR_c\sin\alpha)}{qR_c\sin\alpha}\frac{\sin(qL\cos\alpha/2)}{qL\cos\alpha/2}\right]^2 \sin\alpha\,\mathrm{d}\alpha \quad (5)$$

Cryogenic Transmission Electron Microscopy (cryo-TEM). After a small amount (3−5 μL) of the sample solution was placed on a TEM copper grid covered by a porous carbon film, the excess solution on the grid was blotted with filter paper to form a thin liquid film, and the grid was immediately plunged into liquid propane (−180 °C) cooled by liquid nitrogen in a cryofixation apparatus (LEICA, Reichert KF-80) to fix liquid water as vitreous ice. Then, the ice was transferred into the specimen stage of a cryo-TEM (JEOL, JEM-2100F(G5)) operated at an acceleration voltage of 200 kV through its cryotransfer apparatus cooled by liquid nitrogen. The specimen stage was cooled by liquid helium, and the specimen was kept at −269 °C during observation.

RESULTS AND DISCUSSION

Synthesis. We reacted tris(*N*,*N*-dimethyl-2-aminoethyl)-amine with *n*-alkyl iodides (except for $n = 14$) to obtain the star-type cationic trimeric surfactants in high yields and substitute all three amines. Reactions with *n*-alkyl iodides produced the trimeric surfactants in high yields and less time compared with *n*-alkyl bromides. We tried to measure the surface tension using these trimeric surfactants with iodide counterions; however, they did not dissolve well enough in water, and no breakpoints could be obtained in the surface tension vs concentration plots. Therefore, to improve their water solubility, the counterions of the trimeric surfactants with $n = 8$, 10, and 12 were exchanged with bromide by Dowex 1-X8, and the bromo 3C$_n$trisQs were used in the measurements described below. These star-type trimeric surfactants 3C$_n$trisQ could be obtained in higher yields and more simply than the linear trimeric surfactants (*m*-2-*m*-2-*m*) that we reported previously.[8]

Krafft Temperature and CMC. A clear aqueous solution of star-type trimeric surfactants (0.20 wt %) was prepared by dissolving in hot water and placed in a refrigerator at ∼5 °C for at least 24 h. The temperature of the cooled surfactant solution was then raised gradually under constant stirring, and the conductance (κ) was measured by raising range of 0.5 °C to 1.0 °C. The abrupt change in the κ versus temperature plots was not observed because the Krafft temperatures of star-type trimeric surfactants 3C$_n$trisQ are below 5 °C. The surfactant solutions were clear and showed no precipitates in visual observations. Therefore, the three quaternary ammonium headgroups gave 3C$_n$trisQ good water solubilities at 25 °C despite the three long hydrocarbon chains, even where $n = 14$.

The surface tensions as functions of the concentration for 3C$_n$trisQ with $n = 8$, 10, 12, and 14 at 25 °C were determined and plotted in Figure 2. The surface tensions for $n = 10$, 12, and 14 decreased with increasing concentration, reaching clear breakpoints that were taken to be the CMCs. Unfortunately, for the shortest chain length $n = 8$, the CMC could not be obtained from the plot. In this case, micelles did not form in solution even at the highest concentration studied due to the short chains, and the solution simply became turbid. The surface tension and CMC data were compared to that of the corresponding monomeric, gemini, and linear trimeric surfactants, as listed in Table 1. The data include the CMC, surface tension at the CMC (γ_{CMC}), surface excess concentration (Γ), and area occupied by each surfactant molecule (A). The 3C$_n$trisQ series was compared against monomeric (C$_{12}$TAB; dodecyltrimethylammonium bromide),[5,19] gemini (12-2-12; 1,2-bis(dodecyldimethylammonium)ethane bromide),[5,20] and linear-type trimeric (12-*s*-12-*s*-12; *s* represents spacer chain lengths of 2, 3, and 6) surfactants.[5,7,8] For the $n = 12$ series, 3C$_{12}$trisQ exhibited a CMC value lower than that of the corresponding monomeric and gemini surfactants. It is noteworthy that the CMC decreased by 1 order of magnitude for each additional hydrocarbon chain−hydrophilic headgroup. This signified that the trimeric surfactants had excellent micelle-forming ability at low concentrations because of the increased hydrophobicity provided by three hydrocarbon chains. The CMC of starlike structured 3C$_{12}$trisQ was slightly higher than that of linear 12-2-12-2-12. This was in line with our assumption that 3C$_{12}$trisQ, based on tris(2-aminoethyl)amine, would have greater hydrophilicity because of its tertiary amine. 3C$_{12}$trisQ also exhibited a CMC lower than that of the linear

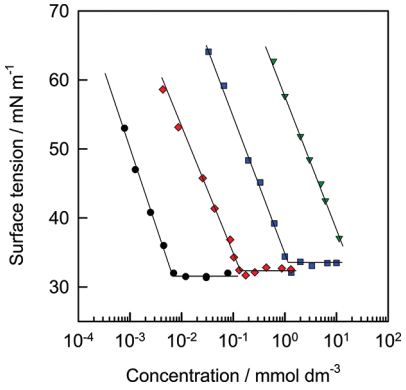

Figure 2. Variation in surface tension with surfactant concentration for 3C$_n$trisQ at 25 °C: ▼ (green), $n = 8$; ■ (blue), 10; ◆ (red), 12; ● (black), 14.

dx.doi.org/10.1021/la301220y | *Langmuir* 2012, 28, 9322−9331

Table 1. The Critical Micelle Concentration, the Surface Tension at the CMC, the Surface Excess Concentration, the Area Occupied per Molecule at the Air/Solution Interface, and the Standard Free Energy of Micellization and Adsorption at the Air/Solution Interface for the Trimeric Surfactants $3C_n$trisQ as well as for Monomeric and Oligomeric Quaternary Ammonium Bromides at 25 °C

surfactant	cmc[a] (mmol dm^{-3})	cmc[b] (mmol dm^{-3})	γ_{cmc} (mN m^{-1})	$10^6\Gamma$ (mol m^{-2})	A (nm^2/molecule)	ΔG°_{mic} (kJ mol^{-1})	ΔG°_{ads} (kJ mol^{-1})
$3C_8$trisQ	–		–	0.875	1.90	–	–
$3C_{10}$trisQ	1.17	1.60	33.4	0.883	1.88	−30.0	−74.0
$3C_{12}$trisQ	0.139	0.177	32.3	0.820	2.03	−36.3	−85.0
$3C_{14}$trisQ	0.00647	0.384	32.1	0.970	1.70	−33.7	−75.0
C_{12}TAB	14[c], 16[d]		38.6[c], 39[d]	3.42[c]	0.49[c]	−18.3	
12-2-12	0.9,[c] 0.967[e]		31.4,[c] 32.4[e]	2.31[c]	0.72,[c] 1.00[c]		
12-2-12-2-12	0.08,[c] 0.065[f]		36.4[f]	1.29,[c] 1.11[f]	1.28,[c] 1.49[f]		
12-3-12-3-12	0.14[g]			1.75[g]	1.47[g]	−64.5[g]	
12-6-12-6-12	0.28[g]			0.7[g]	2.49[g]	−57.0[g]	

[a]Surface tension method. [b]Electrical conductivity method. [c]From ref 5. [d]From ref 19. [e]From ref 20. [f]From ref 8. [g]From ref 7.

cationic trimeric surfactants with spacers such as *trans*-1,4-buten-2-ylene, *m*-xylylene, and *p*-xylylene (0.36, 0.28, and 0.29 mmol dm^{-3}, respectively)[9] and two star-type cationic trimeric surfactants with three amide groups in the spacers (0.20 and 0.33 mmol dm^{-3}),[12] although their counterions were chloride. The plots of hydrocarbon chain length against the logarithm of the CMC of the star-type trimeric surfactants $3C_n$trisQ are compared with monomeric,[17] gemini,[21] and linear-type trimeric[8] surfactants in Figure 3. It is generally known that

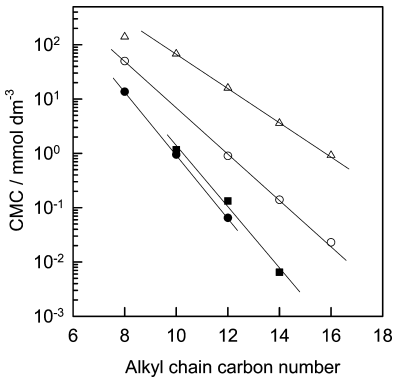

Figure 3. Relationships between the CMC and the hydrocarbon chain length for star-type trimeric $3C_n$trisQ, C_nTAB (monomeric),[17] *n*-2-*n* (gemini),[21] and *n*-2-*n*-2-*n* (linear-type trimeric):[8] ■, $3C_n$trisQ; △, C_nTAB; ○, *n*-2-*n*; ●, *n*-2-*n*-2-*n*.

the CMC decreases logarithmically as the carbon number (n) in the hydrocarbon chain of a homologous series increases, and the relation can be expressed by the so-called Klevens equation as

$$\log \mathrm{CMC} = A - Bn \tag{6}$$

where A and B are constants specific to the homologous series under constant conditions of temperature, pressure, and other parameters. The relationship for star-type $3C_n$trisQ was linear for hydrocarbon chain lengths from 10 to 14, and its slope was quite close to that for the linear-type trimeric series in our previous work. That is, the B values were 0.31, 0.40, 0.58, and 0.56 for C_nTAB, *n*-2-*n*, *n*-2-*n*-2-*n*, and $3C_n$trisQ, respectively. One can see that the B values increased with more chains, indicating that the variation of CMC with the chain length was much larger for trimeric surfactants. However, when the total carbon number in the hydrocarbon chains was taken into account, the effect of chain length on the CMC of the trimeric surfactants was similar to that on gemini, and smaller than that for monomeric ones. The number of chains was plotted against the logarithm of the CMC of each surfactant (C_nTAB, *n*-2-*n*, *n*-2-*n*-2-*n*, and $3C_n$trisQ) for hydrocarbon chain lengths n = 8, 10, 12, and 14 in Figure 4. The relationships between the chain

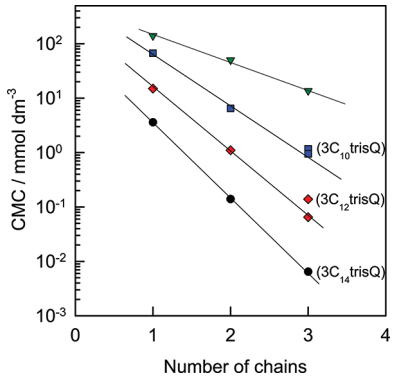

Figure 4. Relationships between the CMC and the hydrocarbon chain length for star-type trimeric $3C_n$trisQ, C_nTAB (monomeric),[17] *n*-2-*n* (gemini),[21] and *n*-2-*n*-2-*n* (linear-type trimeric):[8] ▼ (green), hydrocarbon chain length n = 8; ■ (blue), 10; ◆ (red), 12; ● (black), 14.

number and the logarithm of CMC gave straight lines for the C_nTAB-(*n*-2-*n*)-(*n*-2-*n*-2-*n*) series that have two unit spacers, a phenomenon not described in the previous paper.[8] That is, it can be expressed by the equation

$$\log \mathrm{CMC} = C - Dm \tag{7}$$

where C and D are constants, and m is the number of hydrocarbon chains for analogous surfactants. The D values were 0.51, 0.88, 1.02, and 1.34 for hydrocarbon chain lengths n = 8, 10, 12, and 14, respectively. The change in CMC as more chains were added (slope) increased with chain length. This result was consistent with the fact that micelles form more easily with more hydrophobic surfactants. On the other hand, star-type trimeric surfactants $3C_n$trisQ with n = 10 and 12 deviated from these straight lines. This was probably because $3C_n$trisQ contained one hydrophilic tertiary amine in addition to three quaternary ammonium headgroups in a molecule as described above. This result may also come from the change in the arrangement of three hydrocarbon chains of $3C_n$trisQ molecule at the air/water interface at some critical hydrocarbon chain length which could be 12−14 carbon atoms. This feature is absent in the case of linear-type trimeric surfactants where

dx.doi.org/10.1021/la301220y | *Langmuir* 2012, 28, 9322−9331

the straight orientation of hydrocarbon chains into the hydrophobic phase is present at all hydrocarbon chains. From these data, it was found that the longer the chain length and the more the chain number of surfactants, the lower the CMC. This may be attributed to the thermodynamics, as there was less entropic loss in the formation of micelles of surfactants.[9,22] Thus, we found a relationship between the CMC and the number of chains for a class of cationic surfactants in addition to the Klevens equation that deals with chain length. There has been previous research on the relationship between log CMC and the number of chains for the C_{12}TAB-(12-3-12)-(12-3-12-3-12) series with dodecyl chains and spacer chain length of 3[3] and cationic oligomeric surfactants with dodecyl chains and *trans*-1,4-buten-2-ylene, *m*-xylylene, or *p*-xylylene spacers;[9] however, the linearity was not emphasized. Further studies with other surfactant series will be needed to confirm this relationship.

The CMC obtained by the surface tension method was almost in agreement with that by the electrical conductivity method for $3C_n$trisQ with n = 10 and 12. However, for n = 14, the CMC values obtained using these two methods were not the same. Then, we investigated the CMC of $3C_{14}$trisQ by using the pyrene fluorescence technique. The result showed that the CMC obtained by the fluorescence method was higher than that by the surface tension method and was lower than that by the conductivity method. That is, $3C_{14}$trisQ showed the difference in CMC values by the methods of measurement. One of the reasons may be that the star-type trimeric surfactants with long chains form loose micelles or a premicelle such as a dimer or trimer at the concentrations above the cmc obtained by the surface tension method. This unusual aggregate behavior at low concentration is often observed for the gemini surfactants with long chains. To clarify these properties, further details using small-angle X-ray scattering (SAXS) equipped with powerful X-rays, etc., will be needed.

Adsorption to the Air/Water Interface. The star-type trimeric surfactants in solution required a long time to equilibrium for the surface tension, especially at the concentration below the cmc, and long chain length. The surface tensions at the cmc of star-type trimeric surfactants $3C_n$trisQ with n = 10−14 were 32−34 mN m^{-1}, and they were not dependent on hydrocarbon chain length. $3C_n$trisQ exhibited γ_{CMC} values smaller than those of the corresponding monomeric surfactants, and almost the same γ_{CMC} values as those of the gemini surfactants. The γ_{CMC} values of $3C_n$trisQ were also smaller or almost the same as those of linear-type cationic trimeric surfactants with three dodecyl chains and two spacers such as ethylene (36.4 mN m^{-1}),[8] 2-hydroxypropylene (32 mN m^{-1}),[6] *trans*-1,4-buten-2-ylene, *m*-xylylene, or *p*-xylylene (40−41 mN m^{-1}).[9] This indicated that star-shaped $3C_n$trisQ adsorbed strongly and oriented themselves at the air/water interface. The three hydrocarbon chains, which exist in a ring around tris(2-aminoethyl)amine, facilitated interaction, in contrast with linear surfactants where the hydrocarbon chains of ends separate. As a result, $3C_n$trisQ efficiently lowered the surface tension of water. The surfactants' ability to reduce surface tension is related to their Γ and A. The Γ values of $3C_n$trisQ were smaller and the A values were much larger than those of the corresponding monomeric and gemini surfactants, and they were not independent of hydrocarbon chain length or γ_{CMC}. However, the area occupied by one hydrocarbon chain of $3C_n$trisQ was close to that of a monomeric surfactant. This indicated that the trimeric surfactants adsorbed to the air/water interface and oriented themselves so as to cause high surface activity, due to interactions among the multiple hydrocarbon chains. The star-type $3C_n$trisQ occupied an area slightly more than that of the linear-type trimeric surfactants, because of the differences in the skeletons of tris(2-aminoethyl)amine and diethylenetriamine. Thus, it was found that the star-type trimeric surfactants could adsorb densely at the interface by interactions of the multiple hydrocarbon chains despite the strong electrostatic repulsion between multiple quaternary ammonium headgroups.

These results were also supported by pC_{20} and the CMC/C_{20} ratio, which were proposed by Rosen, and the Gibbs free energy of micellization and adsorption (ΔG°_{mic}, ΔG°_{ads}, respectively). Here, C_{20} is the bulk liquid phase concentration of surfactant required to depress the surface tension of water by 20 mN m^{-1}. The larger the pC_{20} value, the greater the tendency of the surfactant to adsorb at the interface vs forming a micelle in solution. For larger CMC/C_{20} ratios, the adsorption to the surface is easier than forming micelles. For $3C_n$trisQ, the pC_{20} values were 3.9, 5.0, 6.2, and the CMC/C_{20} ratio values were 9.5, 12.4, 9.1 for n = 10, 12, and 14, respectively. The results showed that the pC_{20} and the CMC/C_{20} ratio values of $3C_n$trisQ were much larger than those of most ionic monomeric surfactants where pC_{20} is below 3 and the CMC/C_{20} ratio ranges from 2 to 4.[17] This suggested that adsorption of the present star-type trimeric surfactants is easier than micellization. The ΔG°_{mic} and ΔG°_{ads} of the trimeric surfactants could be obtained from the following equations:[23,24]

$$\Delta G^\circ_{mic} = RT\left(\frac{1}{3} + \beta\right)\ln\left(\frac{CMC}{55.3}\right) - \left(\frac{RT}{3}\right)\ln 3 \quad (8)$$

$$\Delta G^\circ_{ads} = \Delta G^\circ_{mic} - \frac{\pi_{CMC}}{\Gamma} \quad (9)$$

where π_{CMC} denotes the surface pressure at the CMC ($\pi_{CMC} = \gamma_0 - \gamma_{CMC}$, and where γ_0 and γ_{CMC} are the surface tensions of water and the surfactant solution at the CMC, respectively). β is the apparent degree of counterion binding at the micelle/solution interface, calculated from $\beta = 1 - \alpha$ (α is the micelle ionization degree). Here, α is taken to be the ratio of the values of d κ/d C (κ denotes the conductivity) above and below the CMC obtained from the electrical conductivity measurements (Figure 1S in Supporting Information). The α values of $3C_n$trisQ were estimated to be 0.241, 0.224, and 0.504 for n = 10, 12, and 14, respectively. The ΔG°_{mic} and ΔG°_{ads} values of $3C_n$trisQ are also summarized in Table 1. The absolute values of ΔG°_{ads} are significantly greater than those of ΔG°_{mic} for all of the hydrocarbon chain lengths, suggesting that in comparison to micellization, the adsorption of star-type trimeric surfactants is higher.

Kinetics of Adsorption to the Air/Water Interface. To investigate the kinetics of adsorption of star-type trimeric surfactants $3C_n$trisQ to the air/water interface, dynamic surface tension measurements were performed by the maximum bubble pressure technique. These dynamic methods can measure the surface tension in a few milliseconds and are well suited to investigate the kinetics of surfactant adsorption. The variations of surface tension with surface age for $3C_n$trisQ became small, as the hydrocarbon chain length increased from 8 to 12 (Figure 2S in Supporting Information). For n = 14, the dynamic surface tension was close to that of water even for the longest measurement time. This suggested that $3C_{14}$trisQ did not adsorb well for a short time because of steric hindrance caused

dx.doi.org/10.1021/la301220y | *Langmuir* 2012, 28, 9322−9331

by the long hydrocarbon chains in addition to micelle formation in solution. Furthermore, we analyzed the results of the dynamic surface tension with Ward and Tordai's diffusion-controlled adsorption model.[25] The apparent monomer diffusion coefficients (D) could be calculated from long-time dynamic surface tension data by using the Hansen and Joos equation:[26,27]

$$\gamma - \gamma_e = \frac{RT\Gamma^2}{C_0}\sqrt{\frac{\pi}{4Dt}} \quad (10)$$

where γ_e is the equilibrium surface tension at infinite time, γ the dynamic surface tension, Γ the surface excess concentration, which can be obtained from the equilibrium surface tension measurements, C_0 the constant surfactant concentration, and t the time. The plots of γ versus $t^{-1/2}$ based on eq 10 should be linear if the adsorption were diffusion-controlled, allowing the evaluation of D from the slope of the straight line. We plotted surfactant concentration against the D values for $3C_n$trisQ with n = 8, 10, and 12, along with the data from the corresponding monomeric and gemini surfactants (C_{12}TAB, 12-2-12) in Figure 5. The D values of conventional monomeric surfactants

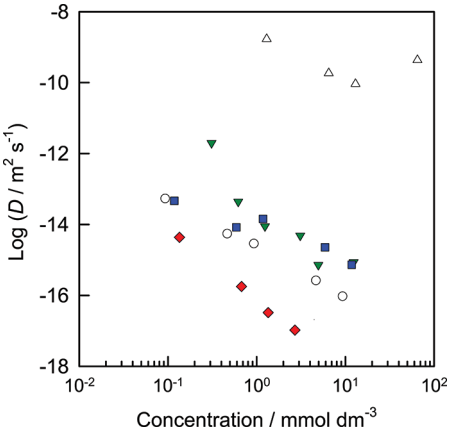

Figure 5. Relationships between diffusion coefficient and surfactant concentration for star-type trimeric $3C_n$trisQ (n = 8, 10, and 12) along with C_{12}TAB (monomeric) and 12-2-12 (gemini) (the diffusion coefficients of C_{12}TAB and 12-2-12 were measured in this study): ▼ (green), $3C_8$trisQ; ■ (blue), $3C_{10}$trisQ; ◆ (red), $3C_{12}$trisQ; △, C_{12}TAB; ○, 12-2-12.

containing C_{12}TAB were on the order of 10^{-10} m^2 s^{-1}. The diffusion coefficient became small by the order C_{12}TAB > $3C_8$trisQ > $3C_{10}$trisQ > 12-2-12 > $3C_{12}$trisQ. Essentially, increasing the degree of oligomerization and the hydrocarbon chain lengths led to a decrease in the kinetics of adsorption at the air/water interface because of increased bulkiness. We attributed this to the adsorption of the surfactant from the subsurface to the interface. The diffusion coefficient of gemini and trimeric surfactants also decreased with increasing concentration, especially above the CMC because of aggregates formed in solution. Miller proposed an adsorption kinetic model that takes into account the formation and dissociation of micelles.[28] Thus, it was found that the star-type trimeric surfactants had slow kinetics of adsorption to the air/water interface.

Rheological Properties in Solution. It is known that rheological behavior depends on the shape of aggregates formed by surfactants in solution.[29,30] The effects of the shape of surfactant aggregates on shear behavior were investigated by rheology measurements. We measured the shear-rate dependence of the viscosity at two concentrations of star-type trimeric surfactants $3C_n$trisQ with n = 10, 12, and 14 and plotted it in Figure 6. Results for pure water were also shown as solid lines

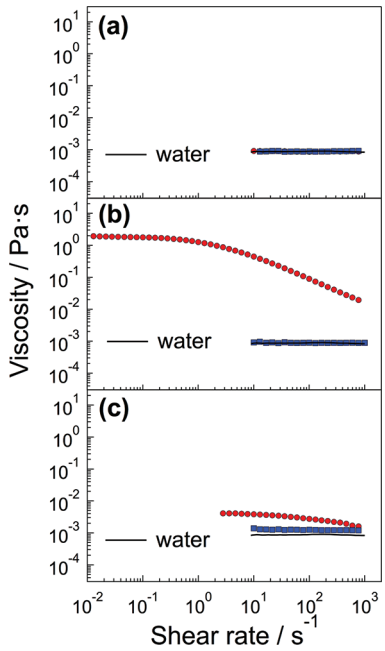

Figure 6. Shear-rate dependence of viscosity for star-type trimeric surfactants $3C_n$trisQ (n = 10, 12, and 14) in aqueous solution: (a) n = 10 (■ (blue), 2.93; ● (red), 5.85 mmol dm^{-3}), (b) n = 12 (■ (blue), 3.48; ● (red), 27.8 mmol dm^{-3}), (c) n = 14 (■ (blue), 0.162; ● (red), 1.62 mmol dm^{-3}).

for reference. For $3C_{10}$trisQ solutions at 2.93 and 5.85 mmol dm^{-3} (2.5, 5.0 times the CMC, respectively), the shear-rate dependence of viscosity was the same as that for water. This was due to aggregation that did not affect solution viscosity. On the basis of the previous findings, we interpreted the shape of the aggregates to be spherical or ellipsoidal micelles.[30,31] For $3C_{12}$trisQ solutions at 3.48 mmol dm^{-3} (25 times the CMC), the viscosity also agreed with that for water, indicating that spherical micelles were formed in solution. As the concentration increased to 27.8 mmol dm^{-3} (200 times the CMC), the viscosity showed a decrease with increasing shear rate, which is known as shear thinning and a typical behavior of rod- or wormlike micelles[32,33] and chainlike polymers.[34] These results implied a spherical micelle-to-rodlike micelle transition as concentration increased. This transition was also observed by using SANS, cryo-TEM, and dynamic viscoelasticity for gemini surfactants with dodecyl chains.[35,36] The details of the spherical micelle-to-rodlike micelle transition for $3C_{12}$trisQ will be described later using SANS and cryo-TEM techniques. For $3C_{14}$trisQ solutions at 0.162 and 1.62 mmol dm^{-3} (25 and 250 times the CMC, respectively), the viscosity was more viscous than water and showed no change as the shear rate increased. The viscosity of $3C_{14}$trisQ was much lower than that of $3C_{12}$trisQ, because of the different concentrations used in measurements for the two surfactants. As the concentration of $3C_{14}$trisQ increases, higher viscosity may be obtained, although it does not dissolve in water.

Structures of Aggregates by SANS and cryo-TEM. SANS is one of the most powerful techniques to quantitatively

dx.doi.org/10.1021/la301220y | Langmuir 2012, 28, 9322−9331

investigate surfactant self-assembly systems in aqueous solution on the nanoscale. SANS measurements were performed to determine the structure of aggregates formed by $3C_n$trisQ with n = 10, 12, and 14 in solution (Figure 7). $3C_{10}$trisQ and

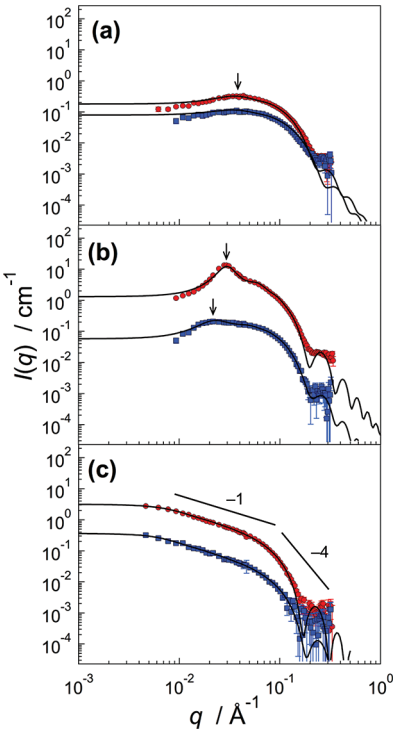

Figure 7. SANS profiles and the fit curves for star-type trimeric surfactants $3C_n$trisQ (n = 10, 12, and 14) in aqueous solution: (a) n = 10 (■ (blue), 2.93; ● (red), 5.85 mmol dm^{-3}), (b) n = 12 (■ (blue), 3.48; ● (red), 27.8 mmol dm^{-3}), (c) n = 14 (■ (blue), 0.162; ● (red), 1.62 mmol dm^{-3}). The solid lines represent the best-fit theoretical scattering functions.

$3C_{12}$trisQ gave peak profiles in the q-range of 0.02 Å^{-1} < q < 0.05 Å^{-1}. These peaks were attributed to repulsive interparticle interactions between the micelles because the micelles were charged on these surfaces. With increasing surfactant concentration, these peak positions (arrows in Figure 7) shifted to higher q values. On the other hand, unlike the case of $3C_{10}$trisQ and $3C_{12}$trisQ, the SANS profiles for $3C_{14}$trisQ had no peaks. That is, the SANS profiles at both concentrations showed $I(q) \sim q^{-1}$ in the low q-range (q < 0.06 Å^{-1}) and $I(q) \sim q^{-4}$ in the high q-range (q > 0.06 Å^{-1}), indicating that $3C_{14}$trisQ formed rod- or wormlike micelles.

The scattering curves were fitted for $3C_n$trisQ with n = 10, 12, and 14 (fit curves in Figure 7). As shown in Figure 6a, the shear-rate dependence of the viscosity indicated that $3C_{10}$trisQ formed spherical or ellipsoidal micelles in solution. Therefore, the theoretical scattering function for charged ellipsoidal particles was fit to a model (eqs 2, 3, and 4). For $3C_{10}$trisQ, the R_1 and u values were estimated to be R_1 = 1.62 nm and u = 0.55 at 2.93 mmol dm^{-3} (2.5 times the CMC), and R_1 = 1.71 nm and u = 0.51 at 5.85 mmol dm^{-3} (5 times the CMC). For $3C_{12}$trisQ, according to the results of the rheological measurements, spherical or ellipsoidal micelles were expected to be also formed at 3.48 mmol dm^{-3} (25 times the CMC). Therefore, the model fit was performed using the scattering function of charged ellipsoidal particles calculated using eqs 2, 3, and 4. By model-fitting analysis, R_1 = 1.93 nm and u = 0.44 were estimated. On the other hand, at 27.8 mmol dm^{-3} (200 times the CMC), the rheological behavior suggested formation of wormlike micelles in solution. Beyond the Guinier q-region, the form factor $P(q)$ for wormlike micelles obeyed the asymptotic behaviors of q^{-2} at a low q-region, q^{-1} at a medium q-region, and q^{-4} at highest q-region. However, the SANS results lacked q^{-2} behavior at a lower q-region. Therefore, using the scattering function of charged rod particles, a model-fitting analysis was performed using eq 5. The structure factor $S(q)$ was calculated using eq 4. The result of the model fitting clearly showed the formation of rodlike micelles with R_c = 2.00 nm and L = 16.61 nm for $3C_{12}$trisQ at 27.8 mmol dm^{-3}.

To confirm the structures of the aggregates formed by $3C_{12}$trisQ, we performed cryo-TEM observations. Cryo-TEM provides a direct visualization of the aggregates present in the thin layers of a vitrified specimen of the solution. Cryo-TEM micrographs for $3C_{12}$trisQ at concentrations of 13.9 and 27.8 mmol dm^{-3} (100 and 200 times the CMC, respectively) are given in Figure 8. We also tried cryo-TEM observations at 6.95 mmol dm^{-3}; however, the micrograph did not clarify due to low concentration. At 13.9 mmol dm^{-3}, threadlike micelles with very few branches were clearly observed, and the length and the number of the micelles increased with increasing concentration. The rod length, L, of the threadlike micelles obtained by the SANS analysis was expected to be approximately the same as the persistence length or mesh size because the cryo-TEM suggested that the micelles had longer contour lengths. Zana et al. reported that linear-type quaternary ammonium salt trimeric surfactants (12-s-12-s-12) form branched threadlike micelles for s = 3[4,7] and spheroidal micelles for s = 6[7] in solution. The shapes of these micelles are also similar to those of the corresponding gemini surfactants 12-s-12 with spacer chain lengths s = 2−12.[35,37] The star-shaped oligomeric surfactants, including $3C_{12}$trisQ, were capable of forming such structures because the multiple hydrocarbon chains of these surfactants could have different relative orientations in the micelles. Furthermore, the strong coulomb repulsions between multiple quaternary ammonium headgroups may have led to an increase in the curvature of the surfactant film, which in turn favors branched threadlike micelles.

For $3C_{14}$trisQ, the SANS profiles pointed to characteristics of rodlike particles at both concentrations. In addition, peak profiles were not observed (i.e., $S(q) \approx 1$). Therefore, model fitting was carried out using only the form factor of the rod particles (eq 5). Through model-fitting analysis, the R_c values were estimated to be 2.26 nm for 0.162 mmol dm^{-3} (25 times the CMC), and 2.13 nm for 1.62 mmol dm^{-3} (250 times the CMC). According to the literature,[38] a scattering profile of rodlike particles indicates the crossover from q^{-1} behavior to constant (i.e., q^0) at the lower q regions (Guinier q-region). However, because this crossover was not observed in the actual SANS results, the length (L) of rodlike micelles for $3C_{14}$trisQ was expected to be more than 25 nm (= $1/q_{min}$, where q_{min} is the lowest accessible q limit). By cryo-TEM, it was confirmed that the rodlike micelles for $3C_{14}$trisQ were threadlike with few branches at 0.324 and 0.648 mmol dm^{-3} (50 and 100 times the CMC, respectively), as shown in Figure 9. Cryo-TEM showed that the branches of threadlike micelles were more for $3C_{14}$trisQ than $3C_{12}$trisQ, while the viscosity of $3C_{14}$trisQ was very low as mentioned above. $3C_{12}$trisQ may form, in practice, threadlike micelles which have further branches, because cryo-TEM is a qualitative method, which is the observation of micelles that may be only a part of the whole

dx.doi.org/10.1021/la301220y | Langmuir 2012, 28, 9322−9331

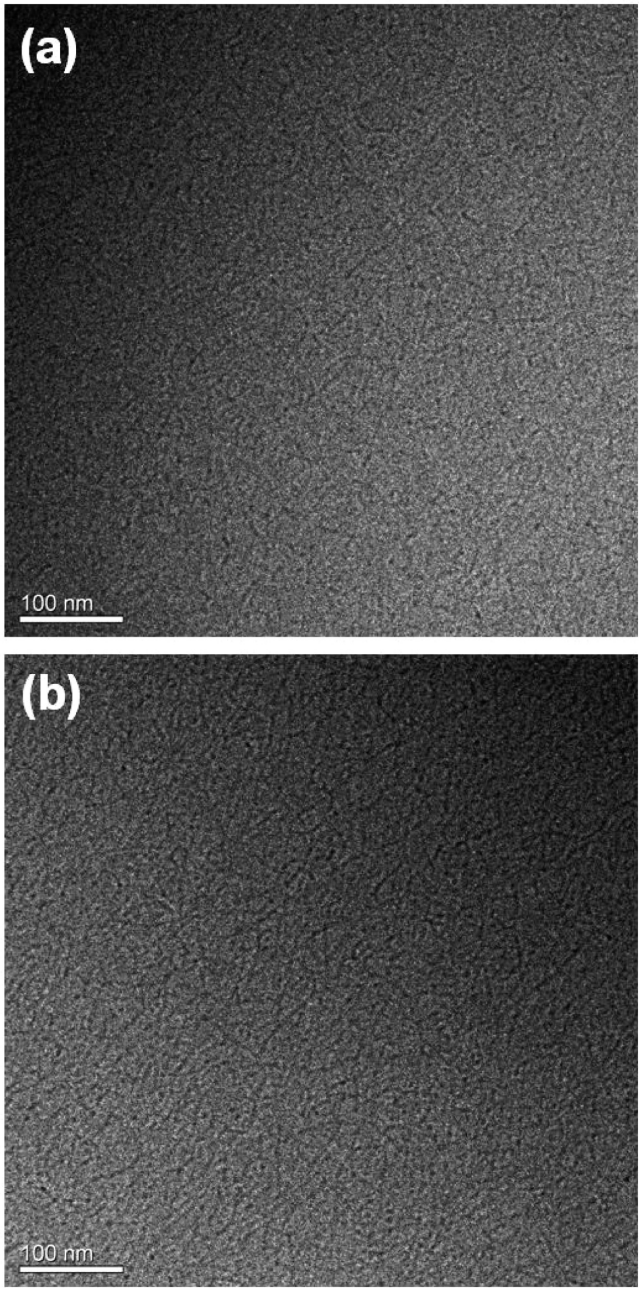

Figure 8. Cryo-TEM images for $3C_{12}$trisQ in solution: (a) 13.9 mmol dm^{-3}, (b) 27.8 mmol dm^{-3}.

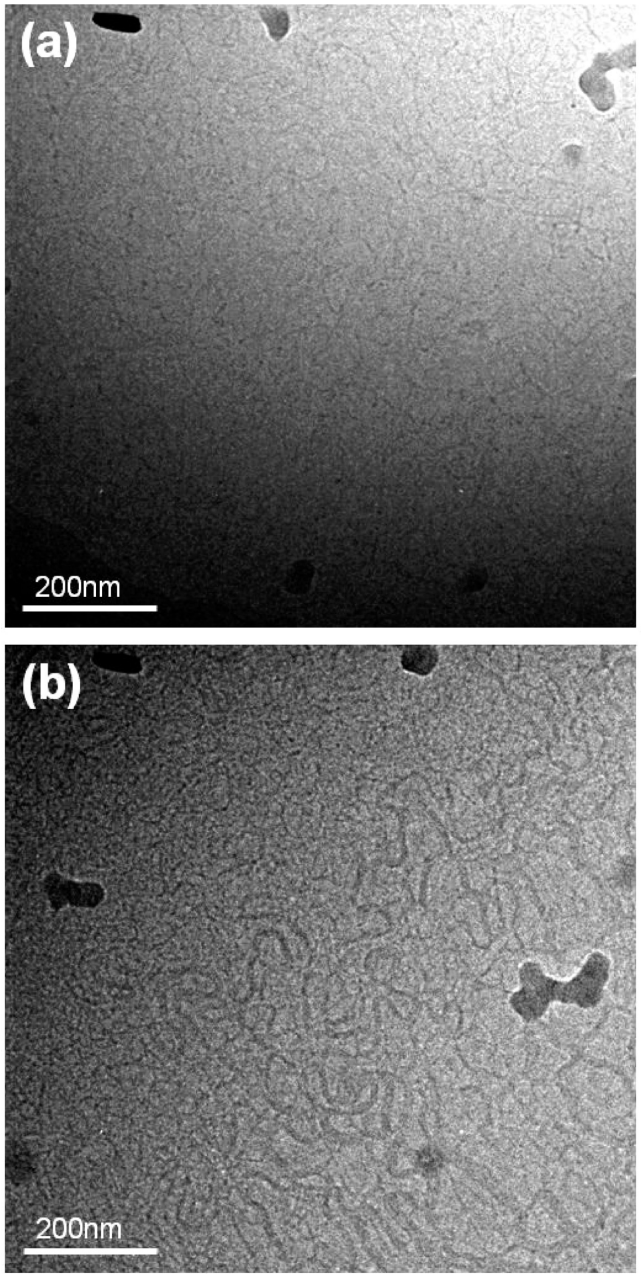

Figure 9. Cryo-TEM images for $3C_{14}$trisQ in solution: (a) 0.324 mmol dm^{-3}, (b) 0.648 mmol dm^{-3}.

system. Thus, it was clarified that the aggregates that formed by the star-type trimeric surfactants $3C_n$trisQ depended on both hydrocarbon chain length and concentration; when they increased, different sequence shapes were observed, from ellipsoidal micelles to threadlike micelles. That is, it was possible to control the shape of the aggregates by changing their factors.

■ CONCLUSIONS

In this article, we designed and synthesized novel star-type cationic trimeric surfactants consisting of three hydrocarbon chains, three quaternary ammonium headgroups, and a tris(2-aminoethyl)amine spacer. We investigated in detail their adsorption and aggregation properties by using various analytical techniques. These surfactants were very soluble in water despite having three hydrocarbon chains in each molecule. The relationship between the logarithm of CMC and hydrocarbon chain lengths was linear as with conventional monomeric and gemini surfactants. We also found a linear relationship between the logarithm of CMC and the number of hydrocarbon chains for linear-type trimeric surfactants with ethylene spacers. Although the adsorption kinetics of trimeric surfactants to the air/water interface was slow, they strongly adsorbed and oriented themselves at the interface, indicating that they lowered the surface tension of water efficiently. The aggregation state of trimeric surfactants in solution was significantly influenced by their hydrocarbon chain lengths and concentrations; that is, for n = 10, ellipsoidal micelle formed, for n = 12, the ellipsoidal micelle changed to threadlike micelles with increasing concentration, and for n = 14,

dx.doi.org/10.1021/la301220y | *Langmuir* 2012, 28, 9322−9331

threadlike micelles formed at low concentration and no transitions were observed as it increased.

Until now, a large number of gemini surfactants have been designed and synthesized by many researchers and their adsorption and aggregation properties investigated. However, there are very few reports for trimeric and tetrameric surfactants, which represent a natural extension of gemini surfactants.[3−16] This is probably because the design and synthesis of oligomeric surfactants such as $3C_n$trisQ are very difficult unlike gemini surfactants, which can be prepared relatively easily. The results in this work may aid future studies of structure−performance relationships for new oligomeric surfactants with novel structures. They will also help to explain the adsorption and aggregation behavior of different types of trimeric surfactants, which have already been reported. We expect to produce further studies on these star-type trimeric surfactants, which were easier to synthesize than expected. These trimeric surfactants should form a new category of surfactants to go along with gemini surfactants.

■ ASSOCIATED CONTENT

Supporting Information

^{1}H NMR and elemental analysis data of synthesized compounds, details of experimental methods, electrical conductivity and dynamic surface tension data of the star-type trimeric surfactants $3C_n$trisQ. This material is available free of charge via the Internet at http://pubs.acs.org.

■ AUTHOR INFORMATION

Corresponding Author

*(T.Y.) E-mail: yoshimura@cc.nara-wu.ac.jp, fax: +81 742 20 3393; (M.S.) E-mail: sibayama@issp.u-tokyo.ac.jp, fax: +81 4 7314 6069.

Notes

The authors declare no competing financial interest.

■ ACKNOWLEDGMENTS

We are grateful to Prof. Hideto Shosenji in the Department of Applied Chemistry and Biochemistry of Kumamoto University for advice of synthesis of surfactants. We also thank Prof. Kunio Esumi in the Department of Applied Chemistry of Tokyo University of Science for many useful suggestions.

■ REFERENCES

(1) Zana, R.; Xia, J. In *Gemini Surfactants: Synthesis, Interfacial and Solution-Phase Behavior, and Applications*; Marcel Dekker: New York, 2004.

(2) Zana, R. In *Structure−Performance Relationships in Surfactants*, 2nd ed.; Esumi, K., Ueno, M.; Marcel Dekker: New York, 2003; Chapter 7, pp 341−380.

(3) Zana, R.; Levy, H.; Papoutsi, D.; Beinert, G. Micellization of two triquaternary ammonium surfactants in aqueous solution. *Langmuir* **1995**, *11*, 3694−3698.

(4) Danino, D.; Talmon, Y.; Levy, H.; Beinert, G.; Zana, R. Branched threadlike micelles in an aqueous solution of a trimeric surfactant. *Science* **1995**, *269*, 1420−1421.

(5) Esumi, K.; Taguma, K.; Koide, Y. Aqueous properties of multichain quaternary cationic surfactants. *Langmuir* **1996**, *12*, 4039−4041.

(6) Kim, T.-S.; Kida, T.; Nakatsuji, Y.; Ikeda, I. Preparation and properties of multiple ammonium salts quaternized by epichlorohydrin. *Langmuir* **1996**, *12*, 6304−6308.

(7) In, M.; Bec, V.; Aguerre-Chariol, O.; Zana, R. Quaternary ammonium bromide surfactant oligomers in aqueous solution: self-association and microstructure. *Langmuir* **2000**, *16*, 141−148.

(8) Yoshimura, T.; Yoshida, H.; Ohno, A.; Esumi, K. Physicochemical properties of quaternary ammonium bromide-type trimeric surfactants. *J. Colloid Interface Sci.* **2003**, *267*, 167−172.

(9) Laschewsky, A.; Wattebled, L.; Arotcaréna, M.; Habib-Jiwan, J.-L.; Rakotoaly, R. H. Synthesis and properties of cationic oligomeric surfactants. *Langmuir* **2005**, *21*, 7170−7179.

(10) Wattebled, L.; Laschewsky, A.; Moussa, A.; Habib-Jiwan, J.-L. Aggregation numbers of cationic oligomeric surfactants: a time-resolved fluorescence quenching study. *Langmuir* **2006**, *22*, 2551−2557.

(11) Hou, Y.; Cao, M.; Deng, M.; Wang, Y. Highly-ordered selective self-assembly of a trimeric cationic surfactant on a mica surface. *Langmuir* **2008**, *24*, 10572−10574.

(12) Wu, C.; Hou, Y.; Deng, M.; Huang, X.; Yu, D.; Xiang, J.; Liu, Y.; Li, Z.; Wang, Y. Molecular conformation-controlled vesicle/micelle transition of cationic trimeric surfactants in aqueous solution. *Langmuir* **2010**, *26*, 7922−7927.

(13) Yoshimura, T.; Esumi, K. Physicochemical properties of ring-type trimeric surfactants from cyanuric chloride. *Langmuir* **2003**, *19*, 3535−3538.

(14) Yoshimura, T.; Esumi, K. Physicochemical properties of anionic triple-chain surfactants in alkaline solutions. *J. Colloid Interface Sci.* **2004**, *276*, 450−455.

(15) Yoshimura, T.; Kimura, N.; Onitsuka, E.; Shosenji, H.; Esumi, K. Synthesis and surface-active properties of trimeric-type anionic surfactants derived from tris(2-aminoethyl)amine. *J. Surfactants Deterg.* **2004**, *7*, 67−74.

(16) Abdul-Raouf, M. E.-S.; Abdul-Raheim, A.-R. M.; Maysour, N. E.-S.; Mohamed, H. Synthesis, surface-active properties, and emulsification efficiency of trimeric-type nonionic surfactants derived from tris(2-aminoethyl)amine. *J. Surfactants Deterg.* **2011**, *14*, 185−193.

(17) Rosen, M. J. *Surfactants and Interfacial Phenomena*, 3rd ed.; John Wiley and Sons: New York, 2004.

(18) Hayter, J. B.; Penfold, J. An analytic structure factor for macroion solutions. *Mol. Phys.* **1981**, *42*, 109−118.

(19) Rosen, M. J.; Mathias, J. H.; Davenport, L. Aberrant aggregation behavior in cationic gemini surfactants investigated by surface tension, interfacial tension, and fluorescence methods. *Langmuir* **1999**, *15*, 7340−7346.

(20) Menger, F. M.; Keiper, J. S.; Mbadugha, B. N. A.; Caran, K. L.; Romsted, L. S. Interfacial composition of gemini surfactant micelles determined by chemical trapping. *Langmuir* **2000**, *16*, 9095−9098.

(21) Zana, R.; Lévy, H. Alkanediyl-α,ω-bis(dimethylalkylammonium bromide) surfactants (dimeric surfactants). Part 6. CMC of the ethanediyl-1,2-bis(dimethylalkylammonium bromide) series. *Colloids Surf., A* **1997**, *127*, 229−232.

(22) Zana, R. Dimeric and oligomeric surfactants. Behavior at interfaces and in aqueous solution: a review. *Adv. Colloid Interface Sci.* **2002**, *97*, 205−253.

(23) Zana, R. Critical micellization concentration of surfactants in aqueous solution and free energy of micellization. *Langmuir* **1996**, *12*, 1208−1211.

(24) Rosen, M. J.; Aronson, S. Standard free energies of adsorption of surfactants at the aqueous solution/air interface from surface tension data in the vicinity of the critical micelle concentration. *Colloids Surf.* **1981**, *3*, 201−208.

(25) Ward, A. F. H.; Tordai, L. Time-dependence of boundary tensions of solutions I. The role of diffusion in time-effects. *J. Chem. Phys.* **1946**, *14*, 453−461.

(26) Hansen, R. S. The theory of diffusion controlled absorption kinetics with accompanying evaporation. *J. Phys. Chem.* **1960**, *64*, 637−641.

(27) Rillaerts, E.; Joos, P. Rate of demicellization from the dynamic surface tensions of micellar solutions. *J. Phys. Chem.* **1982**, *86*, 3471−3478.

(28) Miller, R. Adsorption kinetics of surfactants from micellar solutions. *Colloid Polym. Sci.* **1981**, *259*, 1124−1128.
(29) Afifi, H.; Karlsson, G.; Heenan, R. K.; Dreiss, C. A. Solubilization of oils or addition of monoglycerides derives the formation of wormlike micelles with an elliptical cross-section in cholesterol-based surfactants: a study by rheology, SANS, and cryo-TEM. *Langmuir* **2011**, *27*, 7480−7492.
(30) Takeda, M.; Kusano, T.; Matsunaga, T.; Endo, H.; Shibayama, M.; Shikata, T. Rheo-SANS studies on shear-thickening/thinning in aqueous rodlike micellar solutions. *Langmuir* **2011**, *27*, 1731−1738.
(31) Löf, D.; Schillén, K.; Torres, M. F.; Müller, A. J. Rheological study of the shape transition of block copolymer-nonionic surfactant mixed micelles. *Langmuir* **2007**, *23*, 11000−11006.
(32) Croce, V.; Cosgrove, T.; Maitland, G.; Hughes, T.; Karlsson, G. Rheology, cryogenic transmission electron spectroscopy, and small-angle neutron scattering of highly viscoelastic wormlike micellar solutions. *Langmuir* **2003**, *19*, 8536−8541.
(33) Dreiss, C. A. Wormlike micelles: where do we stand? Recent developments, linear rheology and scattering techniques. *Soft Matter* **2007**, *3*, 956−970.
(34) Goodeve, C. F. A general theory of thixotropy and viscosity. *Trans. Faraday Soc* **1939**, *35*, 342−358.
(35) Danino, D.; Talmon, Y.; Zana, R. Alkanediyl-α,ω-bis-(dimethylalkylammonium bromide) surfactants (dimeric surfactants). 5. Aggregation and microstructure in aqueous solutions. *Langmuir* **1995**, *11*, 1448−1456.
(36) Zana, R.; Talmon, Y. Dependence of aggregate morphology on structure of dimeric surfactants. *Nature* **1993**, *362*, 228−230.
(37) Bernheim-Groswasser, A.; Zana, R.; Talmon, Y. Sphere-to-cylinder transition in aqueous micellar solution of a dimeric (gemini) surfactant. *J. Phys. Chem. B* **2000**, *104*, 4005−4009.
(38) Shibayama, M.; Nomura, S.; Hashimoto, T.; Thomas, E. L. Asymptotic behavior and Lorentz factor for small-angle elastic scattering profiles from preferentially oriented asymmetric bodies. *J. Appl. Phys.* **1989**, *66*, 4188−4197.